



Deposited via The University of Leeds.

White Rose Research Online URL for this paper:

<https://eprints.whiterose.ac.uk/id/eprint/149184/>

Version: Accepted Version

Proceedings Paper:

Bayraktar, F, Benson, AP, Holden, AV et al. (2019) Transcriptomic Approaches to Modelling Long Term Changes in Human Cardiac Electrophysiology. In: Coudière, Y, Ozenne, V, Vigmond, E and Zemzemi, N, (eds.) Lecture Notes in Computer Science. FIMH 2019: Functional Imaging and Modeling of the Heart, 06-08 Jun 2019, Bordeaux, France. Springer Verlag, pp. 3-10. ISBN: 9783030219482. ISSN: 0302-9743. EISSN: 1611-3349.

https://doi.org/10.1007/978-3-030-21949-9_1

© Springer Nature Switzerland AG 2019. This is a post-peer-review, pre-copyedit version of an conference paper published in Functional Imaging and Modeling of the Heart . The final authenticated version is available online at: https://doi.org/10.1007/978-3-030-21949-9_1

Reuse

Items deposited in White Rose Research Online are protected by copyright, with all rights reserved unless indicated otherwise. They may be downloaded and/or printed for private study, or other acts as permitted by national copyright laws. The publisher or other rights holders may allow further reproduction and re-use of the full text version. This is indicated by the licence information on the White Rose Research Online record for the item.

Takedown

If you consider content in White Rose Research Online to be in breach of UK law, please notify us by emailing eprints@whiterose.ac.uk including the URL of the record and the reason for the withdrawal request.

1 Transcriptomic approaches to modelling long term changes in human 2 cardiac electrophysiology

3 Furkan Bayraktar¹, Alan P Benson², Arun V. Holden² and Eleftheria Pervolaraki²

4 ¹ Biomedical Engineering, Afyon Kocatepe University, Afyon, Turkey

5 ² School of Biomedical Sciences, Univ. of Leeds, Leeds LS2 9JT, UK

6 a.v.holden@leeds.ac.uk

7 **Abstract.** Slow changes in the activity of the heart occur with time scales from days through to decades, and
8 may in part result from changes in cardiomyocyte properties. The cellular mechanisms of the cardiomyocyte ac-
9 tion potential have time scales from < ms to hundreds of ms. Although the quantitative dynamic relations between
10 mRNA transcription, protein synthesis, trafficking, recycling, and membrane protein activity are unclear, mRNA-
11 Seq can be used to inform parameters in cell excitation equations. We use such transcriptomic data from a non-
12 human primate to scale maximal conductances in the O'Hara-Rudy (2011) family of human ventricular cell mod-
13 els, and to predict diurnal changes in human ventricular action potential durations. These are related to circadian
14 changes in the incidence of sudden cardiac deaths. Transcriptomic analysis of human fetal hearts between 9 and
15 16 weeks gestational age is beginning to be used to inform ventricular cell and tissue models of the electrophysi-
16 ology of the developing fetal heart.

17 **Keywords:** transcriptomics, circadian, fetal.

18 1 Introduction

19 1.1 Cardiac Excitation Systems

20 Normal sinus rhythm in the human is robust, and persists from 21 days after fertilization until death, maybe 100
21 years later. During the lifetime there can be $\sim 10^9$ beats, each triggered by a propagating excitation wave, at a rate
22 from 40 to 180 beats/min. Noninvasive monitoring of activity of the heart, say by an ECG, show beat to beat
23 fluctuations in the intervals of the cardiac cycles, of the order of tens of ms; accelerations and decelerations of
24 heart rate, lasting $10^1 - 10^2$ s; and longer diurnal, monthly, developmental and ageing changes.

25 A simple computational model of propagating activity in the heart is a nonlinear diffusion system that represents
26 cardiac tissue as mono-domain excitable medium. The nonlinearity is produced by the total membrane ionic cur-
27 rent density I_{tot} ($\mu\text{A}/\mu\text{F}$), given by appropriate excitation equations of the form

$$28 \quad \frac{dV}{dt} = -I_{tot}/C_m, \quad (1)$$

$$29 \quad I_{tot} = I_{ion} + I_{pump} + I_{exchanger} = \mathbf{f}(\mathbf{v}(t), \mathbf{p}),$$

30 where V is the membrane potential (mV), t is the time (ms), $I_{ion} + I_{pump} + I_{exchanger}$ are the ionic, pump and ex-
31 changer current densities and C_m the specific membrane capacitance (μF). The equations for these currents have
32 been obtained from extensive series of voltage clamp experiments on isolated myocytes, and patch clamp exper-
33 iments on recombinant ionic channels expressed in cells. The $\mathbf{v}(t)$ are dynamic variables that change during the
34 solution of the equation, *e.g.* membrane potential, activation and inactivation variables, and some intracellular
35 ionic concentrations. The \mathbf{p} are parameters, some are constants that define the cell type. Some parameters can be
36 changed, to model changes in experimental conditions (*e.g.* temperature, extracellular ionic concentrations).

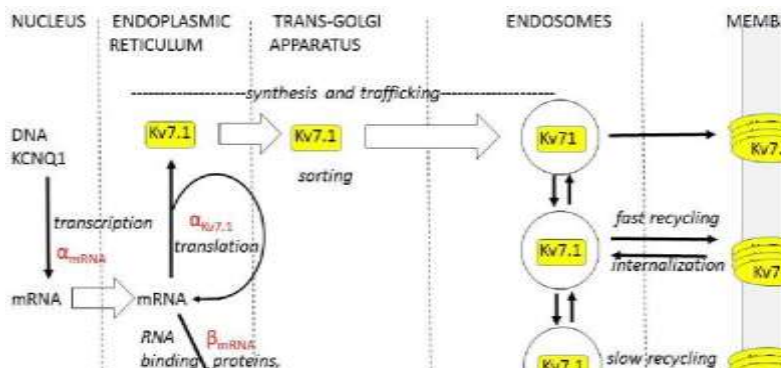
37 We assume that changes in cardiac electrical activity over $10^4 - 10^9$ s in an individual lifetime may be produced
38 by changes in protein expression and can be modelled by changes in the cell population and spatial distributions

42 of these parameters over time. For a human cardiac cell models, the parameters are estimated from experiments
 43 on human cardiac cells and tissue, obtained *ex vivo* during surgery, or from healthy human donor hearts [1].

44 **1.2 Channel expression**

45 In an individual cell, a given specific ion channel density corresponds to a number of functioning channels, each
 46 of which may be composed of several protein subunits and associated regulatory proteins. The number of func-
 47 tioning channels is in a dynamic balance with silent channels, and the total channel number increased by traffick-
 48 ing and insertion to the membrane, and decreased by internalization, recycling and degradation. Proteins newly
 49 synthesized by ribosomes on the endoplasmic reticulum can be transported by endosomes to the membrane. The
 50 dynamics for the alpha subunit of the I_{Ks} channel are schematized in Fig. 1, with α , β the rates of formation and
 51 degradation of the mRNA and protein $Kv7.1$. The overall amount of protein depends on the rate of translation and
 52 degradation [2]: any given steady state level of protein ($\alpha_{mRNA} \cdot \alpha_{Kv7.1} / \beta_{mRNA} \cdot \beta_{Kv7.1}$) could be produced by differing
 53 combinations of transcription [$mRNA\ h^{-1}$] and translation rates [$protein\ mRNA^{-1}\ h^{-1}$]. As well as synthesis and
 54 degradation reactions, there are intracellular transport processes. A compartmental model would be a system of
 55 ordinary differential equations with largely unknown rate coefficients. It is clear that the total amount of mRNA
 56 for the protein subunit, the total amount of the protein subunit, and the ionic maximal conductance G_{Ks} need not
 57 be linearly or even simply related, that there will delays between mRNA, protein and changes in maximal con-
 58 ductance, and that there could be oscillatory or complex dynamics.

59 However, simultaneous measurement by quantitative mass spectrometry of absolute mRNA and protein levels
 60 and half-lives in mouse fibroblasts by pulse labelling has shown a correlation between absolute mRNA and protein
 61 levels in the same samples [3]. This partially justifies approximating the dynamics of Fig.1 by a simple linear
 62 filter, that would give a phase lag and a linear relation between mRNA and maximal conductance.
 63
 64



65
 66
 67 **Fig. 1.** Schematic of the dynamics of the protein alpha subunit $Kv7.1$ of the I_{Ks} channel. Each channel is a tetramer
 68 and the four pore-forming alpha subunits are associated with modulatory $KCNE1$ beta subunits.
 69

70 There are two ways transcriptomics can lead to estimates of the parameters in the cell and tissue excitation equa-
 71 tions.

72 First, where the excitation mechanisms are well described, the transcriptomic data can be taken as quantitative,
 73 and used to scale the values of maximal conductances exchanger, release, and uptake processes of a cell model,
 74 as in [4, 5] for the human sinoatrial node (SAN). The assumption that mRNA expression can be used to scale
 75 maximal conductances was justified by numerical solutions reproducing SAN action potential characteristics.

76 Second, where there are experimental cell electrophysiology recordings, but not a voltage clamp based mech-
 77 anistic model for excitation, the transcriptomic data can be treated as qualitative, to indicate what channel systems

78 are expressed, and the electrophysiological data used to constrain the possible parameter values, as in [6], where
 79 the electro-chemical (membrane potential and intracellular $[Ca^{+}_i]$) activity of single uterine myocytes is recon-
 80 structed. Transcriptomic analysis provides a qualitative list of what mRNAs are expressed [7]. The kinetics of
 81 each ion channel or transporter system is modelled separately, usually from data obtained from patch clamp ex-
 82 periments on an expression system. The assumption is that the kinetics of the channel or transporter in the ex-
 83 pression system used are approximately the same as in the normal cell, even though accessory subunits and
 84 anchoring proteins found in myocytes are not present. Experimentally observed $\{V(t), Ca^{++}(t)\}$ constrain the
 85 space of conductances/densities that are consistent with the observed electrochemistry, and so the cell is modelled
 86 not by a specific set of conductances, but by any member of the space of ionophore densities that is consistent
 87 with the observed $\{V(t), Ca^{++}(t)\}$.

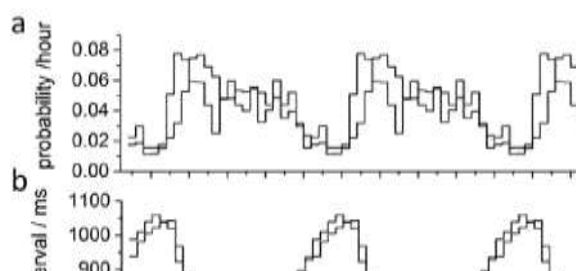
88 1.3 Circadian rhythms

89 Long term, slow diurnal or developmental changes in cardiac activity over 10^4 - 10^9 s will have associated
 90 changes in cardiac myocyte properties and behavior, but longitudinal or population transcriptomic and cellular
 91 electrophysiological studies over these time scales are impractical. Computational modelling of human cell and
 92 tissue electrophysiology, informed by the limited available transcriptomic data, may suggest possible cellular
 93 electrophysiological changes that could provide the mechanisms for these changes in activity. Here we approach
 94 the modeling of circadian (10^4 s) and fetal developmental (10^6 s) from 9 to 16 weeks gestational age (WGA).

95 Cardiac electrophysiological variables – heart rate, ECG intervals and their variability, and the onset of ar-
 96 rhythmia, all show diurnal rhythms [8]. The timing of sudden cardiac deaths, obtained from out of hospital and
 97 in-hospital data [9, 10], and of the onset of ventricular fibrillation, obtained from ICD data downloads [11], both
 98 show a diurnal rhythm - see Fig.2a. The time is local clock time. The four-fold change in sudden cardiac death
 99 rates has a rise time of ~ 6 hours and a fall time of ~18 hours. The rhythms for sudden cardiac death, onset of
 100 ventricular tachycardia and fibrillation are mirrored by the diurnal changes in RR interval [12, 13] – see Fig 2b.
 101 These diurnal rhythms in heart rate and SCD could be driven by external factors or autonomic activity [14], or
 102 could be generated by circadian changes in ion channel expression within the heart [8] that are entrained, *via*
 103 autonomic and humoral factors, by the suprachiasmatic nucleus that provides synchronization to the daylight
 104 [15].

105 Diurnal changes in heart rate will produce rate dependent changes in ventricular action potential duration, dis-
 106 persion, and variability that provide an obvious possible explanation for diurnal changes in SCD. Any intrinsic
 107 diurnal changes in myocyte membrane channel expression could directly modulate the risk of SCD.

108
109



110
111
112 **Fig. 2.** Circadian changes in cardiac events, averaged over 10^3 - 10^4 subjects and several years. (a) Replot of SCD
 113 data from Berlin, $n=2406$ [9], ; Massachusetts ($n=2203$ [10]). (b) Average RR interval for normal adult subjects,
 114 replot from [12, 13].

115
116

1 1 7 2 Methods

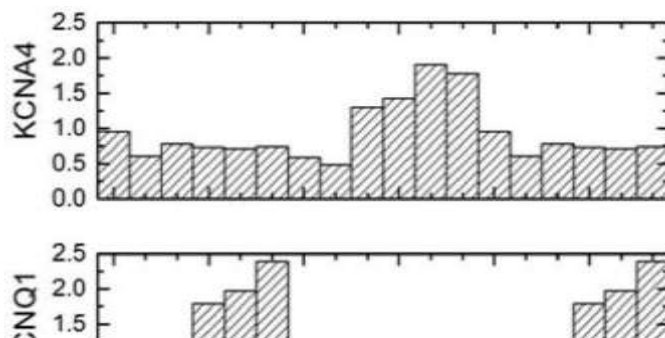
118 An extensive diurnal transcriptome atlas of the transcriptome of different tissues for the primate *Papio anubis*
 119 (baboon) on a 12 hour light-12 hour dark cycle has been published and archived in NCBI's GEO (GSE98965)
 120 [16]. 12 animals were used, to give 12 time points every 2 hours *i.e* one animal /time point. 15% of the cardiac
 121 transcriptome products shows a diurnal rhythm, with the times of peak expression clustered in a temporal window
 122 <6 hrs wide, and periodicity identified by meta2d of Metacycle [17]. Transcriptomics data was extracted for
 123 the α -subunits proteins that form part of the membrane ionic channels for the inward currents I_{Na} (SCN5A), $I_{Ca,L}$
 124 (CACNA1C) and outward currents I_{to} (KCND3,KCNA4), I_{Kur} (KCNA5), I_{Kr} (KCNH2), I_{Ks} (KCNQ1) and I_{K1}
 125 (KCNJ2/12/4), $I_{K,ACh}$ (KCNJ3/5), $I_{K,ATP}$ (KCNJ11). Only changes in KCNA4 and KCNQ1 are statistically signif-
 126 icant (Metacycle integrated $p < 0.05$). The gene level read counts are normalized.

127 Fetal developmental changes in mRNA for cardiac ion channel protein were extracted from the data [18]
 128 deposited in European Genome-Phenome Archive (EGA) which is hosted at the EBI and the CRG, (E-MTAB-
 129 7031) for time points 9, 12 and 16 WGA, with each time point being the average from 3 hearts.

130 The percentage change in mRNA were used to scale the ionic conductances in the O'Hara-Rudy [19] model
 131 for human healthy ventricular cells. Equations for isolated cell models were solved using a forward Euler method
 132 with a time step of $\Delta t = 0.05$ ms; ion channel gating equations were solved using the Rush-Larsen scheme. The
 133 action potential duration at 90% repolarization (APD_{90}) restitution was measured using a standard protocol, with
 134 100 S1 pacing beats at a cycle length of 1,000 ms to establish periodicity, followed by a single premature stimulus
 135 (S2) at progressively shorter S1-S2 intervals

1 3 6 3 Results

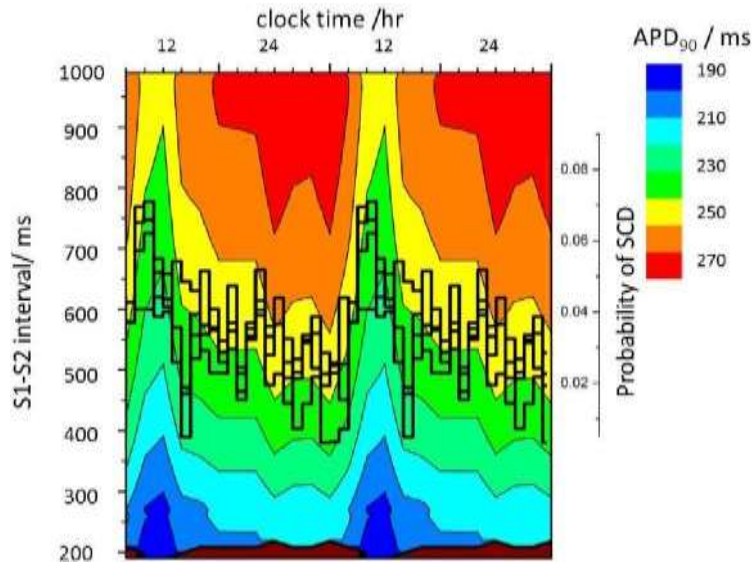
137 *Circadian changes.* The normalized individual gene level read counts are plotted for KCNA4 and KCNQ1 in
 138 Fig.3. The Zeitgeber time (ZT) relates to the 24 hour light-dark cycle, with light on at ZT=0. Each 2 hour wide
 139 column over 24 hours in the histogram is based on one animal, and the observation that there are compact peaks,
 140 at different times for the two mRNAs, suggests that the modulation is related to ZT and not the individual animal.
 141 When the G_{to} and G_{Kr} are scaled by the normalized channel expression data of Fig.3 there is a diurnal modulation
 142 of APD_{90} and its restitution. This is plotted in Fig. 4 over 48 hours, with S1-S2 intervals from 200 to 1000ms,
 143 with APD_{90} colour-coded over for each 2 hour time window of the day. Light on (ZT0) is identified as the
 144 average local clock time of dawn over the year (6 *a.m.*), and the diurnal pattern of sudden cardiac death of Fig.2(a)
 145 is superimposed. There appears to be a coincidence between the diurnal pattern of APD_{90} and the timing of
 146 SCD's.



147
 148 **Fig. 3.** Diurnal changes over 36 hours in cardiac ion channel expression in baboons that had been entrained on a
 149 24 hours (12 hour light, 12 hour dark) cycle.

150

151



152

153

154

155

156

Fig. 4. Circadian changes in ventricular endocardial cell model dynamic APD_{90} restitution curves, computed using data in Fig.3. The sudden cardiac death rates from Fig 2 are superimposed, with ZT0 (light on) taken as 06.00 a.m. APD_{90} is colour-coded.

157

158

159

Developmental changes. The development of ventricular structure, intercellular coupling, and transcriptome in the human fetus has been mapped from 9 to 20 WGA by DT-MRI [20, 21], RNA-Seq [18] and qPCR[20], and related to noninvasive electrophysiology [21].

160

161

162

163

164

165

166

The organization of the ventricular wall, quantified by fractional anisotropy, apparent diffusion coefficients and fiber paths lengths extracted by tractography, increases linearly with gestational age, with the helical organization, and transmural change in fiber helix angle characteristic of the adult mammalian heart developed by 20 weeks. RNAseq showed no significant differential expression of Cx40 or Cx 43 between 9 and 16 WGA [18], while both Cx 40 and Cx43 expression relative to GAPDH obtained by Western blotting increased significantly [20]. The increase in organisation correlates with an increase in Connexin expression [20]. In tissue models these increase both propagation velocity and its anisotropy.

167

168

169

170

171

172

173

Differential expression of genes coding ion channel subunits has been extracted from the data of [18]; of the 806 genes differentially expressed between 9 and 16 WGA) only 20 relate to cardiac excitation with potassium voltage-gated channel (KCNJ2, KCNJ2-AS1,KCTD9,KCNJ8), sodium voltage-gated channel (SCN2B,SCN7A), gap junction protein alpha (GJA1, GJA3) and ryanodine receptor 2 (RYR2), all upregulated; and potassium voltage-gated channel and modifiers KCNAB3, KCNA1, KCNG1, KCNQ2);calcium voltage-gated channels (CACNG4, CACNG7, CACNA1G/H/S), potassium calcium activated channel (KCNN1) and Ryanodine receptor RYR2 all downregulated.

174

175

176

177

178

179

180

The ORD model is parameterized for the healthy adult, and there are no well-founded, experimentally based models of human fetal myocardial cells whose parameters could be scaled by the transcriptomic data. In [21, 22] conductance parameters of an adult endocardial myocyte model were scaled so their APD_{90} restitution curves reproduce 35 week gestational age fetal QT restitution curve. The transcriptomic data would give an increase in maximal rate of rise of action potential, and increase in its conduction velocity and duration, but quantitative values are speculative in the absence of fetal cell and tissue electrophysiological data. However, transcriptomics of *ex-vivo* or *postmortem* material could be applied to the ORD system to model ageing in the adult.

181 4 Conclusions

182 Transcriptomic data provides a route to parameterizing human cardiac excitation equations to reproduce slow
 183 developmental changes, seen over time scales of days to decades, time scales that are not accessible for cell and
 184 tissue electrophysiology. What is needed is a clearer, quantitative description of the dynamics of transcription and
 185 membrane protein synthesis: the first order approximation of a linear relation between mRNA level and functional
 186 membrane ionophore activity is oversimplified, even though it leads to plausible behaviors.

187

188 Acknowledgements.

189

190 F.B. was supported by an ERAMUS + traineeship.

191 References

- 192 1. Holzem, K.M., Madden, E.J., Efimov, I.R.: Human cardiac systems electrophysiology and arrhythmogenesis. *Europace*.
 193 16 Suppl 4:iv77-iv85. (2014).
- 194 2. Curran J., Mohler, P.J. Alternative paradigms for channelopathies. *Ann. Rev. Physiol.* 77 505-24 (2015).
- 195 3. Schwanhäusser, B. *et al.* Global quantification of mammalian gene expression control. *Nature* 473, 337–342 (2011).
- 196 4. Chandler, N.J., *et al.* Molecular architecture of the human sinus node: insights into the function of the cardiac pacemaker
 197 *Circulation*. 3; 119(12):1562-75. (2009)
- 198 5. Boyett, M.R. ‘And the beat goes on’ The cardiac conduction system: the wiring system of the heart. *Experimental Physi-*
 199 *ology* 94:(10) 1035-1049 (2009).
- 200 6. Atia, J., *et al.*, Reconstruction of Cell Surface Densities of Ion Pumps, Exchangers, and Channels from mRNA Expression,
 201 Conductance Kinetics, Whole-Cell Calcium, and Current-Clamp Voltage Recordings. *PloS Comput Biol.* 22;
 202 12(4):e1004828 (2016).
- 203 7. Chan, Y. *et al.*, Assessment of myometrial transcriptome changes associated with spontaneous human labour by high-
 204 throughput RNA-seq. *Exp Physiol* 99(3): 510–524 (2014).
- 205 8. Black, N., *et al.* Circadian rhythm of cardiac electrophysiology, arrhythmogenesis, and the underlying mechanisms *Heart*
 206 *Rhythm*Feb;16(2):298-307 (2018)
- 207 9. Arntz, H-R., *et al.* Diurnal, weekly and seasonal variation of sudden death. *Eur Heart J.* 21 (4) (2000).
- 208 10. Willich, S.N. *et al.* Circadian Variation in the Incidence of Sudden Cardiac Death in the Framingham Heart Study Popula-
 209 tion. *Am. Journal of Cardiology.* 60 (10): 803-804 (1987).
- 210 11. Tofler, G.H., *et al.*, Morning peak in ventricular tachyarrhythmias detected by time of implantable cardioverter/defibrillator
 211 therapy. *Circulation* 92:1203–1208 (1995).
- 212 12. Gang, Y *et al.*, Circadian variation of the ST interval in patients with sudden cardiac death after myocardial infarction.
 213 *American J. of Cardiology*, 81, pp. 950-956, (1998)
- 214 13. Bonnemeier H. *et al.*, Circadian Profile of Cardiac Autonomic Nervous Modulation in Healthy Subjects: Differing Effects
 215 of Aging and Gender on Heart Rate Variability *J Card-iovacular. Electrophysiology* Vol. 14, pp. 791-799 (2003)
- 216 14. West *et al.* Misalignment with the external light environment drives metabolic and cardiac dysfunction. *Nature Communi-*
 217 *cations* 18:417 DOI: 10.1038/s41467-017-00462-2
- 218 15. Crnko S. *et al.* Circadian rhythms and the molecular clock in cardiovascular biology and disease. *Nature Rev. Cardiology*
 219 2019 Feb 22. doi: 10.1038/s41569-019-0167-4 (2019)
- 220 16. Mure, L.S. *et al.*, Diurnal transcriptome atlas of a primate across major neural and peripheral tissues. *Science* 359, eaao0318
 221 (2018).
- 222 17. Wu, G *et al.* MetaCycle: An integrated R package to evaluate periodicity in large scale data. *Bioinformatics* 32, 3351–
 223 3353 (2016).
- 224 18. Pervolaraki, E. *et al.*, The developmental transcriptome of the human heart. *Sci Rep.* Oct 18; 8(1):15362 (2018).
- 225 19. O'Hara, T., Virag, L., Varro, A., Rudy, Y. Simulation of the undiseased human cardiac ventricular action potential. *PLOS*
 226 *Computational Biology* 7, e1002061 (2011).
- 227 20. Pervolaraki E, Dachtler J, Anderson RA, Holden AV. Ventricular myocardium development and the role of connexins in
 228 the human fetal heart. *Sci Rep.* 2017 Sep 25;7(1):12272
- 229 21. Pervolaraki E, *et al.* Antenatal architecture and activity of the human heart. *Interface Focus.* 2013 Apr 6; 3(2):20120065.
 230 doi: 10.1098/rsfs.2012.0065.

231 22. Pervolaraki E, Hodgson S, Holden AV, Benson AP. Towards computational modelling of the human foetal electrocardi-
232 ogram: normal sinus rhythm and congenital heart block. *Europace*. 2014 May; 16(5):758-65. doi: 10.1093/euro-
233 pace/eut377.